

Elsevier Editorial System(tm) for Geoderma
Manuscript Draft

Manuscript Number:

Title: Combining seismic and electric methods for predicting bedrock depth along a Mediterranean soil toposequence

Article Type: Research Paper

Section/Category: Pedometrics

Keywords: diachronic electrical resistivity tomography; spectral analysis of surface waves; bedrock depth; shallow groundwater; vineyard

Corresponding Author: Mr. Guillaume COULOUMA,

Corresponding Author's Institution: INRA

First Author: Guillaume COULOUMA

Order of Authors: Guillaume COULOUMA; Kevin SAMYN; Gilles GRANDJEAN; Stéphane FOLLAIN; Philippe LAGACHERIE

Abstract: Bedrock depth provides important information for many environmental and agricultural applications, such as shallow groundwater monitoring, the determination of soil water availability, and the estimation of crop production potential. Direct estimates of bedrock depth from destructive soil observations are discontinuous and too expensive to be used in large areas. Geophysical methods are often cited as possible alternatives. However, their ability to provide reliable estimations of bedrock depth is known to depend greatly on local site characteristics. Therefore, combining geophysical methods based on different physical parameters may help to provide better predictions. This study examines the ability of the Spectral Analysis of Surface Waves (SASW) method combined with the classical high resolution Electrical Resistivity Tomography (ERT) method to predict soil depths in a 500 m ranged Mediterranean hillslope (Southern France) with increasing soil depths along the slope. SASW was performed using the data measured in the field with classical seismic equipment (impulse source and geophones distributed along a line). In the same place, eight transects of ERT (Wenner-Schlumberger array, 1 m electrode spaced) were measured under wet and dry conditions. To calibrate the geophysical measurements, 81 boreholes (from two to five metres deep) were interpreted to determine the bedrock depth, which was defined as the occurrence in the depth of heterogeneous marine Miocene loose sandstone with centimetric laminations. ERT and SASW were found to have highly variable performances for predicting separately the bedrock depth along the hillslope. SASW correctly predicted the bedrock depth in the lower part of the hillslope, whereas the data from ERT were disrupted by shallow permanent groundwater. Conversely, ERT correctly predicted bedrock depth within the upper part of the hillslope, whereas a high variability of SASW data near the topsoil caused difficulties for bedrock depth prediction. From these results, it was possible to define an estimator of bedrock depth according to the presence of shallow groundwater, which varies along the slope, such that more importance is given to ERT estimates in the upper part of the hillslope and more importance is given to SASW in the lower part. This study shows the usefulness of such a sensor combination to estimate soil properties when the uncertainties of making predictions vary according to the geophysical methods.

Guillaume COULOUMA
corresponding author
INRA, UMR LISAH
2 place Viala
34060 MONTPELLIER CEDEX 1

Montpellier, 10th of may

to editorial board of Geoderma

Dear editorial board,

On behalf of the authors, please find enclosed the manuscript : "Combining seismic and electric methods for predicting bedrock depth along a Mediterranean soil toposequence" to be submitted to Geoderma.

In this manuscript, we propose a new combination of methodologies recently applied to soil science for predicting bedrock depth. This soil property is an important issue in soil science and few works have evaluated it either by classical or newer methodologies.

In order to verify the English language of our paper, we submitted this manuscript to American Journal Expert (please find enclosed the certificate of English review)

we hope that you 'll agree on the interest of this work.

Kind regards

Guillaume Coulouma, corresponding author



www.journalexperts.com

American Journal Experts Editorial Certification

This document certifies that the manuscript titled "Combining seismic and electric methods for predicting bedrock depth along a Mediterranean soil toposequence" was edited for proper English language, grammar, punctuation, spelling, and overall style by one or more of the highly qualified native English speaking editors at American Journal Experts. Neither the research content nor the authors' intentions were altered in any way during the editing process.

Documents receiving this certification should be English-ready for publication - however, the author has the ability to accept or reject our suggestions and changes. To verify the final AJE edited version, please visit our verification page. If you have any questions or concerns over this edited document, please contact American Journal Experts at support@journalexperts.com

Manuscript title: Combining seismic and electric methods for predicting bedrock depth along a Mediterranean soil toposequence

Authors: Coulouma, G., Samyn, K., Grandjean, G., Follain, S. and Lagacherie, P.

Key: 7288-A8BC-A989-DCB2-85BA

This certificate may be verified at www.journalexperts.com/certificate

American Journal Experts is an association of Ph.Ds and Ph.D. graduate students from America's top 10 research universities. Our editors come from nearly every research field and possess the highest qualifications to edit research manuscripts written by non-native English speakers. We provide the quickest turnaround times at the lowest prices in the industry. For more information, please visit www.journalexperts.com, or for volume discounts for academic journals, please contact us by email at sales@journalexperts.com

Highlights

- Bedrock depth is an important issue in soil science.
- A new seismic methodology (SASW) and diachronic ERT were tested to predict bedrock depth (BD) in Mediterranean vineyards.
- Diachronic ERT predicted BD in shallow soils.
- SASW predicted BD in deeper soils despite the presence of groundwater.
- A combination of these methodologies along the toposequence enhanced the prediction of BD.

Abstract

Bedrock depth provides important information for many environmental and agricultural applications, such as shallow groundwater monitoring, the determination of soil water availability, and the estimation of crop production potential. Direct estimates of bedrock depth from destructive soil observations are discontinuous and too expensive to be used in large areas. Geophysical methods are often cited as possible alternatives. However, their ability to provide reliable estimations of bedrock depth is known to depend greatly on local site characteristics. Therefore, combining geophysical methods based on different physical parameters may help to provide better predictions. This study examines the ability of the Spectral Analysis of Surface Waves (SASW) method combined with the classical high resolution Electrical Resistivity Tomography (ERT) method to predict soil depths in a 500 m ranged Mediterranean hillslope (Southern France) with increasing soil depths along the slope. SASW was performed using the data measured in the field with classical seismic equipment (impulse source and geophones distributed along a line). In the same place, eight transects of ERT (Wenner-Schlumberger array, 1 m electrode spaced) were measured under wet and dry conditions. To calibrate the geophysical measurements, 81 boreholes (from two to five metres deep) were interpreted to determine the bedrock depth, which was defined as the occurrence in the depth of heterogeneous marine Miocene loose sandstone with centimetric laminations. ERT and SASW were found to have highly variable performances for predicting separately the bedrock depth along the hillslope. SASW correctly predicted the bedrock depth in the lower part of the hillslope, whereas the data from ERT were disrupted by shallow permanent groundwater. Conversely, ERT correctly predicted bedrock depth within the upper part of the hillslope, whereas a high variability of SASW data near the topsoil caused difficulties for bedrock depth prediction. From these results, it was possible to define an estimator of bedrock depth according to the presence of shallow groundwater, which varies along the slope, such that more importance is given to ERT estimates in the upper part of the hillslope and more importance is given to SASW in the lower part. This study shows the usefulness of such a sensor combination to estimate soil properties when the uncertainties of making predictions vary according to the geophysical methods.

1. Introduction

1
2
3 A major physical and chemical discontinuity can be observed between the regolith and
4 geologic material without weathering features, which constitutes “bedrock” (Brimhall et al.,
5 1991; Ma et al., 2010). Bedrock generally constitutes an impermeable layer of shallow
6 groundwater. For plants, bedrock depth (BD) is often indicative of the rooting limit (Shenk,
7 2008) and this knowledge is significant for determining the shape of a root system (Ganatsas
8 & Spanos, 2005; Shenk & Jackson, 2002), soil water availability and crop production
9 potential. Moreover, describing the bedrock geometry is essential to defining the limits of the
10 outline of the Critical Zone (Brandley et al., 2006).

11
12 Although the knowledge of BD remains an important issue in the soil sciences, few studies
13 have evaluated it either by using classical or newer methodologies. Direct estimates of BD
14 from destructive boreholes and pits are too expensive to be used in large areas, but
15 geophysical methods appear to be a possible non-invasive alternative. Classical Electrical
16 Resistivity tomography (ERT) is used to determine BD when there are highly contrasted
17 resistivity levels between the soil layers and bedrock, as significant technological
18 improvements have increased its spatial resolution. Beauvais et al. (1999) characterised the
19 geometry of the soil layers above high-resistivity granitic bedrock using ERT. In the same
20 way, irregular BDs in karst terranes were measured by ERT, taking advantage of high contrast
21 of resistivity between the clayey soil and limestone (Zhou et al., 2000). More recently,
22 Beauvais et al. (2007) mapped the weathering of ultramafic rocks with a combination of ERT
23 and geomorphologic parameters. Another way to predict bedrock consists of studying
24 diachronic ERT to determine the water uptake localisation. Some other studies have also
25 shown the possibility of using diachronic ERT (Brunet et al., 2010; Descloîtres et al., 2008;
26 Michot et al., 2003; Nitjland et al., 2010). Srayeddin & Doussan (2009) showed the suitability
27 of using diachronic ERT for mapping and quantifying the water uptake of maize and sorghum
28 crops after calibration with conventional monitoring. However, the efficiency of ERT was
29 decreased when bedrock exhibited poor resistivity contrasts with the upper soil layers
30 (Coulouma et al., 2010). In the case of saturated porous media, such as shallow groundwater,
31 the ERT signal becomes independent from the soil and bedrock’s electrical properties.
32 Therefore, there are complex situations for which poor resistivity contrasts between soil layers
33 and bedrock or the presence of shallow groundwater have been observed.

34
35 Besides ERT, seismic methods are not currently used in the soil sciences but could be
36 particularly promising to solve these problems. Due to the development of subsurface
37
38
39
40
41
42
43
44
45
46
47
48
49
50
51
52
53
54
55
56
57
58
59
60
61
62
63
64
65

1
2
3
4
5
6
7
8
9
10
11
12
13
14
15
16
17
18
19
20
21
22
23
24
25
26
27
28
29
30
31
32
33
34
35
36
37
38
39
40
41
42
43
44
45
46
47
48
49
50
51
52
53
54
55
56
57
58
59
60
61
62
63
64
65

characterisation studies for environmental or geotechnical purposes, the efficiency of seismic methods for estimating ground velocity structures and mechanical properties has progressed in recent decades and has found various applications in several fields, such as waste disposal (Lanz et al., 1998), landslides (Grandjean et al., 2007), and hydrogeophysics (Sturtevant et al., 2004). Recent equipment, generally containing 48 or 72 recording channels and PC-piloted acquisition software, has made this method operational and contributed to its dissemination. A few years ago, an adaptation of the sensor line, based on unplugged gambled geophones, was proposed to reduce drastically acquisition times (Grandjean, 2006a; Debeglia et al., 2006). This improvement was also supported by the development of new data processing protocols like acoustical tomography (Azaria et al., 2003; Grandjean, 2006b) or the Spectral Analysis of Surface-waves (SASW) (Grandjean and Bitri., 2006; Park et al., 2000) and related multichannel applications (MASW) (Foti, 2000; Miller, 1999; Park et al., 1999a, 1999b; Xia et al., 1999). The MASW method allows one to assess the shear resistance of materials and was recently used to determine bedrock depth in contrasting areas and assess the soil's vulnerability to erosion (Samyn et al., 2011). Combining different geophysical methodologies using fuzzy logic data fusion was also used to enhance the efficiency of BD prediction (Grandjean et al., 2007). The aim of this paper is to present a combined approach of classical geophysical methodologies, namely geoelectrical and seismic methods, in the complex case of the presence of shallow groundwater and poorly contrasting bedrock. In particular, this study examines the ability of classical high-resolution diachronic ERT combined with the MASW methodology to predict BD in a 500 m ranged agricultural Mediterranean hillslope.

2. Site description

The study area is located in a Mediterranean climate area that is 60 km west of Montpellier (southern France) on the 0.91 km² Roujan catchment (43°30'N, 3°19'E). The mean annual rainfall of 650 mm is irregularly distributed throughout the year, and the major periods of rainfall occur in spring and autumn. The mean temperature is approximately 14°C. The substratum of the catchment is a loose and heterogeneous Miocene marine sandstone with centimetric laminations and intercalations of loamy clay material. This sandstone constitutes the bedrock of the studied toposequence (Figure 1). The soils (IUSS Working Group WRB, 2006) along the toposequence are directly developed over the Miocene loose sandstone with a spatial distribution that depends on the location within the slope. The distribution is i) calcaric

1 regosols in the upper part of the hillslope, which is sandy silt textured and described by a high
2 calcium carbonate content; ii) calcisols in the middle part of the hillslope; and iii) endogleyic
3 calcisols at the bottom part of the hillslope. At the slope scale, the soils are characterised by
4 an increase in soil depth and a change in soil texture in relation to the colluvial accumulations
5 of clay and gravels. The main characteristics of the soils are summarised in Table 1.
6
7

8
9 <Table 1 here>

10 In the lower part of the catchment, shallow groundwater developed in a high porosity horizon
11 (aquiferous horizon) overlays the sandstone. The maximum piezometric level of the
12 groundwater is shown in Figure. 1. Two situations can be distinguished in the toposequence;
13 in the lower part, the groundwater is found within the soil layers, whereas, in the upper part,
14 the groundwater is below the soil and partly in the sandstone.
15
16
17
18

19
20 <Figure 1 here>

21 22 23 24 25 26 27 28 29 30 31 32 33 34 35 36 37 38 39 40 41 42 43 44 45 46 47 48 49 50 51 52 53 54 55 56 57 58 59 60 61 62 63 64 65

hal-00657824, version 1 - 9 Jan 2012

3. Materials and methods

3.1 Geological and pedological measurements

<Figure 2 here>

In March 2009, 81 boreholes (2-5 m deep) were made to describe the soil profiles and to determine the BD (Figure 2). Each borehole was described according to the STIPA system (Falipou & Legros, 2002) for soil horizonation. Bedrock was found in only 36 boreholes when the drilling was deep enough to reach it. The morphological parameters were observed in the field (texture, structure, colour, stone and classes of calcium carbonate content); BD was also estimated in relation to these descriptions. The criteria for bedrock identification were the presence of (i) a lamellar structure without macropores, (ii) a hue of 2.5Y or 5Y, (iii) silty or sandy texture and (iv) no gravels or signs of colluvial redistributions. Groundwater signs were annotated in each borehole and additional monitoring of the water table was performed in eight piezometers to validate the presence of groundwater signs with the observation data. Observed groundwater was delimited for each section and checked in relation to the monitored piezometers.

3.2 Geophysical measurements

3.2.1 Seismic measurements

<Figure 3 here>

The SASW method is a recently conceived seismic method used to determine shear wave velocity (V_s) models. Measurements are performed directly at the soil surface without invasive action, allowing for less expensive measurements than for conventional drilling surveys. The main principle of the method uses the dispersive properties of surface-waves (Park et al., 2000), meaning that each wave frequency component travels at a different velocity. Smaller and larger wavelengths are influenced by the seismic velocities of shallower and deeper parts of the subsurface, respectively. Because these dispersion effects can be measured in seismic data, the V_s model – V_s variations with depth – that produced them can be estimated using seismic data inversion theory. To obtain a reliable V_s model, three steps are necessary: (1) seismic acquisition (Figure 3a); (2) the determination of the experimental dispersion curves, i.e., the surface-waves phase velocity (V_{ph}) variation with frequency (Figure 3b); and (3) the inversion of the experimental dispersion curves to obtain the variation of V_s with depth (Figure. 3d).

For step (1), data were acquired along eight linear transects (Figure 2) in June 2009. To obtain a more convenient and better estimation the dispersion curves, we used an MASW. Samyn et al. (2011) discussed the adaptation of the MASW method to soil investigation. It consisted of 24 takeouts with a 0.5 m interval. Each takeout was attached to a single, self-orientating, gimbals-mounted, vertical geophone that was able to record signals from 10 to 200 Hz frequencies (Figure 3b). To help ensure proper coupling, each gimbal geophone was housed in a heavy casing (~1 kg). To damp the motion of the sensor around its rotational axis, the inside of the casing was filled with a viscous oil. The entire system was towed behind a vehicle to ensure an optimal time acquisition. A 24-channel Geometrics Geode seismograph was used to record the impacts of a hammer source that was able to generate signals in the ones to few tens of Hz frequency range. During recording, the wavefield was discretised and truncated in both the time and space domains. The sampling periods in the time domain were 0.5 ms, and there were 1000 samples taken. The near offset (distance between the source point and the first recording point along the line) was 0.5 m, the geophone spacing was 0.5 m, and the offset range is 11.5 m (Figure 3a).

For Step (2), we processed the seismic data to identify wave dispersion. A 2D wavefield transform method is commonly used to determine experimental dispersion curves. This processing involves a 2D wavefield operation that transforms the seismic data from the space-

hal-00657824, version 1 - 9 Jan 2012

1
2
3
4
5
6
7
8
9
10
11
12
13
14
15
16
17
18
19
20
21
22
23
24
25
26
27
28
29
30
31
32
33
34
35
36
37
38
39
40
41
42
43
44
45
46
47
48
49
50
51
52
53
54
55
56
57
58
59
60
61
62
63
64
65

time domain into the frequency-phase velocity domain, which is more convenient for highlighting the dispersion features (McMechan and Yedlin, 1981). The dispersion curve is then defined as the maximum peaks in the transformed domain (Figure. 3b).

Step (3) is meant to solve the inverse problem. It is used to find the parameters that best characterise the soil layers (here, V_s value and the thicknesses of layers) from dispersion curves that were estimated in Step (2). These curves are compared to predicted ones and create residuals in the least square sense, which are minimised during the resolution of the inverse problem (Tarantola, 1987) (Figure 3c). This resolution consists of adjusting a set of soil model parameters – typically V_s and the thickness values of each layer – that offer the minimum residuals. In general, seismic inverse problems are non-linear, but they can be solved by iterative schemes (Tarantola, 1987). The inverse algorithm used in our study implements all these aspects and is based on the work of Hermann (1987). The stop criterion was defined for V_{ph} residuals as less than 5 m/s. Figure 3d shows a V_s model, representing a layered V_s structure, obtained using an inversion process of the dispersion curve in Figure 3b-c.

3.2.2 Electrical measurements

2D Electrical Resistivity Tomography (ERT) sections were made along the same eight transects in February 2009 in wet conditions and in August 2009 in dry conditions. ERT measurements were performed using a Wenner-Schlumberger array with an electrode spacing of 1 m. We used 50 electrodes simultaneously on each transect to provide the apparent electrical resistivity over the profile at ~0.5 m increments down the profile until reaching a maximum depth of 5 m. The electrical resistivity for each soil layer and bedrock was derived from the apparent electrical resistivity measurement using an inverse method, i.e., the Gauss-Newton code Res2dinv as described by Locke (2002). The electrical resistivity depended on the temperature at the time of the measurement as well as on the water content, porosity, conductivity of the soil solution and the mineralogy of the soil particles (Telford et al., 1990). To compare the two ERT surveys, at different dates on the same field, the resistivity values were corrected to a standard temperature of 25°C, using the following equation by Keller and Frischknecht (1966): $\rho_{25} = \rho_T \cdot [1 + \alpha(T - 25)]$ where ρ_T is the electrical resistivity ($\Omega \cdot m$) from the measured apparent electrical resistivity at temperature T , ρ_{25} is the electrical resistivity ($\Omega \cdot m$) at a standard temperature $T = 25^\circ$, and α is a constant equal to 0.02 for a temperature range of 5-25°C.

1
2
3
4
5
6
7
8
9
10
11
12
13
14
15
16
17
18
19
20
21
22
23
24
25
26
27
28
29
30
31
32
33
34
35
36
37
38
39
40
41
42
43
44
45
46
47
48
49
50
51
52
53
54
55
56
57
58
59
60
61
62
63
64
65

The temperatures were monitored at the piezometers at every metre of depth during the electrical resistivity measurements. The results were fitted to obtain a corrected temperature for each depth step and for each date of resistivity measurements.

3.3 Bedrock depth prediction from ERT

Water content, porosity in the first tilled horizon and the conductivity of the soil solution were parameters that were susceptible to change between the two dates of the electrical surveys. Only changes in the water content can significantly modify the electrical resistivity at a standard temperature (Besson et al., 2010; Michot et al., 2003). Electrical resistivity values measured for dry and wet conditions were plotted against soil depth at every metre of the eight transects. These punctual ERT data were analysed to define the BD hypothetically corresponding to the depth until no significant differences of resistivity between dry and wet conditions were observed (Figure 4b). The significant differences were attributed to (i) the vine water uptake between the wet period at the beginning of the vegetal activity and the dry one at the maximum of the vegetal activity and (ii) the drainage out of the soil system. The limit between the soil and bedrock represent a discontinuity in hydraulic conductivity and in vine rooting depth, modifying the shape of a root system that is known to be larger than that of other crops (Soar & Lovey, 2007; Trambouze & Voltz, 2001). From each electrical data point, BD was then predicted as the depth beyond which no significant differences in electrical resistivity were observed between the wet and dry conditions (Figure. 4a). However, in the case of deep soils, the assumed hypothesis for BD prediction appears to be incorrect in relation to the presence of the groundwater system (Figure 1) and to the effective vine rooting depth, which is lower than the actual soil depth.

<Figure 4 here>

3.3 BD prediction from MASW

Vs are very sensitive to the mechanical properties of the soil skeleton and less so to the water content. They range from very low values as low as 15 m.s⁻¹ in extremely loose clays to more than 1000 m.s⁻¹ in consolidated materials. Therefore, they are able discriminate well between loose and competent materials (Puech et al., 2004). In general, MASW data points indicate a low-velocity coverage layer (around 150-200 m.s⁻¹) with a 1 to 4-5 m thickness according to the location in the toposequence. Further down, the velocities increased with depth and

reached 400 m.s^{-1} , indicating a more competent material that has assimilated to the underlying bedrock (Figure 4a). From each seismic data point, BD was predicted on the 1D vertical Vs profiles considering the inflexion point between the low-velocity coverage layer and the high-velocity underlying layer (Figure 4b).

4. Results and discussion

4.1 Measured BD

Figure 5 shows the observed BD and groundwater level from the boreholes and piezometers along the eight transects. The median of observed BD was 1.7 m with significant differences along the slope. Bedrock outcrops were generally localised at the topslope position of the toposequence, whereas one outcrop was located in the middle part of the west hillslope. BDs greater than three metres were only observed in the lower part of the hillslope.

The water tables observed in the boreholes on the date of the soil measurements were classified in relation to their presence within the soil. Water tables are always present within the soil in the lower part of the hillslope where soils are deeper than two metres (Figures 1-5). The observed water tables were in agreement with the monitored piezometric data.

<Figure 5 here>

4.2 Resistivity of the soil layers and bedrock

<Figure 6 here>

At each borehole location, the temperature-corrected resistivity values for the wet and dry conditions were categorised according to the main soil layers and bedrock. Figure 6 shows that the mean resistivity values did not exceed $50 \Omega.m$. The observed range of the values was similar to previous measurements recorded for the same soil and bedrock types (Telford et al. 1990). In the tilled horizons, the standard deviation and maximum values showed significant variability due to differences in soil structure (Coulouma et al., 2006) and in soil type (Andrieux et al., 1993). The same behaviour was observed in the bedrock due to differences in bedrock type, e.g., within or without centimetric lamination of loamy clay material. The lower mean resistivity value logically corresponds to an aquiferous layer that is saturated throughout the year.

1
2
3
4
5
6
7
8
9
10
11
12
13
14
15
16
17
18
19
20
21
22
23
24
25
26
27
28
29
30
31
32
33
34
35
36
37
38
39
40
41
42
43
44
45
46
47
48
49
50
51
52
53
54
55
56
57
58
59
60
61
62
63
64
65

No significant differences in resistivity were found between soil layers or tilled horizons and bedrock under both conditions. Differences in resistivity between both conditions in tilled horizons and soil layers can be attributed to the water dynamics in the vadose zone. A single analysis of the resistivity values does not allow us to exploit the differences in water dynamics between the soil and bedrock, which is believed to be one possible way to determine BD.

4.3 BD prediction

4.3.1 Contribution of each methodology

<Figure 7 here>

The observed BDs that were determined from boreholes were compared to ones predicted from the ERT analysis (Figure 7a). A very low determination coefficient was observed for the entire dataset ($R^2=0.08$). In the case of the presence of groundwater, BDs were underestimated by the ERT analysis. These estimated BDs probably correspond to the depth of vine water uptake that was limited by root development in relation to the presence of a capillary fringe near the water table level. Conversely, ERT analysis was effective when not in the presence of groundwater.

Measured BDs from boreholes were also compared to ones predicted by the MASW method (Figure 7b). A very low determination coefficient was also observed for the entire dataset ($R^2=0.13$). BDs were overestimated in conditions of reduced soil depth. This overestimation was due to the lack of high frequencies that are required for the characterisation of the shallowest materials. Conversely, the MASW method was not deterred by the presence of groundwater. In fact, Vs are sensitive to the properties of the soil skeleton and less so to the water content, whereas the ERT signal was disrupted by the groundwater.

4.3.2 Combined methodologies

The results allow us to define the applicability of each methodology at the scale of the toposequence based on the presence of groundwater within the soil. According to their applicability, the combined BD was derived by the BD predicted from ERT in the absence of groundwater and from MASW in the presence of groundwater. A buffer zone of 20 metres centred on the limit was defined because of the difficulties in making accurate delimitations for the presence or absence of groundwater. Within this buffer zone, weighted means of the

1 predicted BD for each methodology were calculated to define a combined BD in relation to
2 the distance from the limit. BDs predicted from the combination of ERT and MASW analysis
3 were then compared to the observed BDs (Figure. 8). Utilising this combination significantly
4 improved the estimation of BD ($R^2=0.77$).
5
6

7 <Figure 8 here>
8

9 Continuous geophysical measurements allowed us to estimate BD based on the presence of
10 observed groundwater for the entire geophysical dataset using the ERT and MASW
11 combination. Figure 9 shows the results of the BD prediction for each geophysical transect.
12 The general trend of shallow soils at the top of the hillslope and increasing soil depth down
13 the slope is consistent with the observations of Figure. 5. However, BD varied strongly along
14 the toposequence. Outcrops of bedrock are generally localised on the top of the hillslope
15 (between 250 and 300 m from the bottom of the hillslope) except in three outcrops (between
16 150 and 180 m from the bottom of the hillslope). The irregular shape of the BD predicted
17 from the MASW method at short intervals did not represent the actual features of the bedrock
18 because of the 1D hypothesis used in the seismic inversion process, which was independent
19 from the closest predictions. Conversely, the BD predicted from ERT analysis showed a
20 regular bedrock shape, which was made possible by the 2D integrator inversion process of
21 electrical resistivity. It is likely that this corresponded better to the actual shape of the
22 bedrock. Complementary data processing, such as smoothing operations of the bedrock shape
23 in relation to geomorphologic information, are necessary to provide the realistic shape of the
24 bedrock along the entire toposequence. Nevertheless, we conclude that the general
25 distribution of the predicted BDs is likely to be a reasonable first-order approximation of the
26 actual situation in the subsurface.
27
28
29
30
31
32
33
34
35
36
37
38
39
40
41

42 <Figure 9 here>
43
44

45 **4.4 Discussion**

46
47
48

49 The detection of bedrock using geophysical methods depends greatly on the definition of the
50 bedrock and the bedrock's properties. ERT is generally used in contrasted areas, such as
51 clayey soils developed over limestone (Zhou et al., 2000) or weathered soils over magmatic
52 materials (Beauvais et al., 2007), when significant differences in electrical resistivity between
53 bedrock and soil are evident. In our case, the contrast in resistivity between calcisols and
54 heterogeneous loose sandstone was not sufficient to determine the limit between soil and
55
56
57
58
59
60
61
62
63
64
65

1 bedrock. Since the first successful use of diachronic ERT, analysing the pattern of the water
2 uptake by a grapevine has constituted an alternative way of determining the limit of bedrock
3 in vineyard areas. However, this methodology is not efficient in the presence of groundwater.
4 Combining it with a sensor that is based on another physical parameter greatly enhances
5 bedrock detection. Therefore, seismic surface waves have great potential for discriminating
6 between loose and compact materials and are not sensitive to the water content despite poor
7 BD prediction in the case of shallower soils. This hypothesis is founded on the presence of
8 laminations, which correspond to marine sedimentation processes. This is considered to be a
9 criterion for bedrock determination in conventional measurements. These laminations
10 increase the differences in hardness between soil and bedrock. In addition, the effects of this
11 limit on rooting depth and soil hydraulic conductivity have been verified in boreholes and pits
12 (Andrieux et al., 1993; Coulouma et al., 2006).

13 Figure 8 shows BDs estimated from a combination of the ERT and MASW methodologies.
14 The MSE (0.24 m) of the prediction is acceptable but higher than in previous studies on
15 bedrock estimation directly from diversified geophysical methodologies (Gerber et al., 2010;
16 Zhou et al., 2000). Other works have estimated BDs from soil databases or DEM with larger
17 RMSE results (Dalke et al., 2009; Ziadat, 2010). However, the experimental conditions of
18 this study were chosen specifically in relation to (i) the difficulty in defining bedrock in the
19 case of loose bedrock and poorly contrasted materials and (ii) the variability of bedrock
20 properties and depth along the toposequence. Even better results are expected from a
21 combination of the ERT and MASW methods for BD prediction in more contrasted
22 environments. Samyn et al. (2011) discussed the feasibility of calibrating shear wave
23 velocities using penetrometer soundings to increase the accuracy of BD prediction using
24 seismic surface waves and the accuracy of a combined BD prediction. This calibration should
25 improve the relation observed between Vs and soil layers defined from pedological
26 parameters to determine a hypothetical threshold corresponding to bedrock shear wave
27 velocity.

28 Finally, the applicability of each methodology is based on the presence of groundwater within
29 the soil. This information is not readily available and requires shallow groundwater
30 monitoring. An alternative is to use soil morphological indicators of saturation that could help
31 in detecting and mapping water tables (Tassinari et al., 2002). However, this study only
32 provides information regarding the applicability of the tested methodologies; it is possible to
33 use other indicators, such as topographical ones (from DEM) and pedological ones that are
34
35
36
37
38
39
40
41
42
43
44
45
46
47
48
49
50
51
52
53
54
55
56
57
58
59
60
61
62
63
64
65

1
2
3
4
5
6
7
8
9
10
11
12
13
14
15
16
17
18
19
20
21
22
23
24
25
26
27
28
29
30
31
32
33
34
35
36
37
38
39
40
41
42
43
44
45
46
47
48
49
50
51
52
53
54
55
56
57
58
59
60
61
62
63
64
65

either derived from ground observed morphological indicators of saturation (Tassinari et al., 2002) or from an available soil map.

5. Conclusion

This study examines bedrock detection in the regularly encountered complex situations of loose bedrocks with the possible presence of shallow groundwater. An expensive and discontinuous drilling approach was compared with classical ERT and a new application of SASW. ERT and SASW separately provide insufficient bedrock detection at the scale of a 500 metre-ranged toposequence. However, an analysis of diachronic data combined with SASW at the scale of the toposequence enhanced the efficiency of bedrock detection according to the presence of shallow groundwater. Bedrock detection can be improved by using easily calculated geomorphological or topographical parameters as indicators of the efficiency of each geophysical methodology. However, this combination of methodologies according to prior soil knowledge must be tested in different representative soils.

Acknowledgements

This study was funded by the FP7-DIGISOIL project and the French ANR-VMCS LANDSOIL project. The DIGISOIL project (FP7-ENV-2007-1 N°211523) is financed by the European Commission under the 7th Framework Programme for Research and Technological Development, Area “Environment”, Activity 6.3 “Environmental Technologies”. In particular, the authors thank E. Dupuits, F. Garnier, A. Rochat and J.L. Belotti for their help with the field work.

References

- Andrieux, P., Bouzigues, R., Joseph, C., Voltz, M., Lagacherie, P., Bourlet, M., 1993. Le bassin versant de Roujan : caractéristiques du milieu. UR Science du Sol, INRA, Montpellier, France.
- Azaria, A., Zelt, C., Levander, A., 2003. High-resolution seismic mapping at a groundwater contamination site: 3-D travelttime tomography of refraction data. EGS-AGU-EUG Joint Meeting, Nice, France.

- 1
2
3
4
5
6
7
8
9
10
11
12
13
14
15
16
17
18
19
20
21
22
23
24
25
26
27
28
29
30
31
32
33
34
35
36
37
38
39
40
41
42
43
44
45
46
47
48
49
50
51
52
53
54
55
56
57
58
59
60
61
62
63
64
65
- Besson, A., Cousin, I., Bourennane, H., Nicoullaud, B., Pasquier, C., Richard, G., Dorigny, A., King, D., 2010. The spatial and temporal organization of soil water at the field scale as described by electrical resistivity measurements. *European J. of Soil Science* 61,120-132.
- Beauvais, A., Ritz, M., Pariscot, J. C., Dukhan, M., Bantsimba, C., 1999. Analysis of poorly stratified lateritic terrains overlying a granitic bedrock in West Africa using 2-D electrical resistivity tomography. *Earth and Planetary Science Letters* 173, 413-424.
- Beauvais, A., Parisot, J.C., Savin, C., 2007. Ultramafic rock weathering and slope erosion processes in a South West Pacific tropical environment. *Geomorphology* 83, 1-13.
- Brantley, S.L., White, T.S., White, A.F., Sparks, D., Richter, D., Pregitzer, K., Derry, L., Chorover, O., April, R., Anderson, S., Amundson, R., 2006. *Frontiers in Exploration of the Critical Zone*. National Science Foundation Workshop. October 24-26, 2005, Newark, USA.
- Brimhall, G.H., Lewis, C.J., Ford, C., Bratt, J., Taylor, G., Warin, O., 1991. Quantitative geochemical approach to pedogenesis – Importance of parent material reduction, volumetric expansion and eolian influx in lateritization. *Geoderma* 51, 51-91.
- Brunet, P., Clement, R., Bouvier, C., 2010. Monitoring soil water content and deficit using ERT – A case study in the Cevennes area, France. *Journal of Hydrology* 380, 146-153.
- Coulouma, G., Boizard, H., Trotoux, G., Lagacherie, P., Richard, G., 2006. Effect of deep tillage for vineyard establishment on soil structure: A case study in Southern France. *Soil Till Res* 88, 132-143.
- Coulouma, G., Tisseyre, B., Lagacherie, P., 2010. Is a Systematic Two-Dimensional EMI Soil Survey Always Relevant for Vineyard Production Management? A Test on Two Pedologically Contrasting Mediterranean Vineyards, in : Viscarra Rossel, R.A., McBratney, A., Minasny, B. (Eds.), *Proximal soil sensing*. Progress in Soil Science series, Springer, New York, pp. 283-295.
- Dahlke, H.E., Behrens, T., Seibert, J., Andersson, L., 2009. Test of statistical means for the extrapolation of soil depth point information using overlays of spatial environmental data and bootstrapping techniques. *Hydrol. Process.* 23, 3017-3029.
- Debeglia, N., Bitri, A., Thierry, P., 2006. Karst investigations using microgravity and MASW: Application to Orléans, France. *Near Surface Geophysics* 4, 215-225.
- Descloîtres, M., Ruiz, L., Sekhar, M., Legchenko, A., Braun, J.J., Mohan Kumar, M.S., Subramanian, S., 2008. Characterization of seasonal local recharge using ERT and magnetic resonance sounding. *Hydrol. Process* 22, 384-394.

- 1
2 Falipou, P., Legros, J.P., 2002. Le système STIPA-2000 d'entrée et édition des données pour
3 la banque nationale de sols DONESOL II. *Etude et Gestion des Sols* 9, 55-70.
- 4 Foti, S., 2000. Multistation Methods for Geotechnical Characterization using Surface-waves,
5 Dottorato di Ricerca in Ingegneria Geotecnica.
- 6
7 Ganatsas, P., Spanos, I., 2005. Root system asymmetry of Mediterranean pines. *Plant and Soil*
8 278, 75-83.
- 9
10 Gerber, R., Felix-Henningsen, P., Behrens, T., Scholten, T., 2010. Applicability of ground-
11 penetrating radar as a tool for non-destructive soil-depth mapping on Pleistocene
12 periglacial slope deposits. *J. Plant Nutr. Soil Sci.* 173, 173-184.
- 13
14 Grandjean, G., Bitri, A., 2006. 2M-SASW inversion of local Rayleigh wave dispersion in
15 laterally heterogeneous subsurfaces: application to Super-Sauze earthflow, France.
16 *Near Surface Geophysics* 4, 367-375.
- 17
18 Grandjean, G., 2006a. A seismic multi-approach method for characterizing contaminated
19 sites. *J. Applied Geophys.* 58, 87-98.
- 20
21 Grandjean, G., 2006b. Imaging subsurface objects by seismic P-wave tomography: numerical
22 and experimental validations. *Near Surface Geophysics* 4, 275-283.
- 23
24 Grandjean, G., Malet, J.P., Bitri, A., Meric, O., 2007. Geophysical data fusion by fuzzy logic
25 for imaging mechanical behaviour of mudslides. *Bull. Soc. Geol. France* 177, 133-
26 143.
- 27
28 Hermann, R.B., 1987. Computer programs in seismology. Saint-Luis University, USA.
- 29
30 Hunter, J.A., Benjumea, B., Harris, J.B., Miller, R.D., Pullan, S.E., Burns, R.A., Good, R.L.,
31 2002. Surface and downhole shear wave seismic methods for tick soil site
32 investigations. *Soil dynamics and Earthquake Engineering* 22, 931-941.
- 33
34 IUSS Working Group WRB, 2006. World reference base for soil resources 2006. 2nd edition.
35 World Soil Resources Reports No. 103. FAO, Rome.
- 36
37 Keller, G.V., Frischknecht, F.C., 1966. *Electrical Methods in Geophysical Prospecting.*
38 Pergamon Press, Oxford.
- 39
40 Lanz, E., Mauer, H., Green, A.G., 1998. Refraction tomography over a buried waste disposal
41 site. *Geophysics* 63, 1414-1433.
- 42
43 Loke, M.H., 2002. Tutorial: 2D and 3D electrical imaging surveys. Technical note 2nd ed.
44 Malaysia.
- 45
46 Ma, L., Chabaux, F., Pelt, E., Blaes, E., Jin, L., Brantley, S.L., 2010. Regolith production
47 rates calculated with uranium-series isotopes at Susquehanna/Shale Hills Critical Zone
48 Observatory. *Earth and Planet. Sci. Lett.* 297, 211-225.
- 49
50
51
52
53
54
55
56
57
58
59
60
61
62
63
64
65

- 1
2
3
4
5
6
7
8
9
10
11
12
13
14
15
16
17
18
19
20
21
22
23
24
25
26
27
28
29
30
31
32
33
34
35
36
37
38
39
40
41
42
43
44
45
46
47
48
49
50
51
52
53
54
55
56
57
58
59
60
61
62
63
64
65
- Michot, D., Benderitter, Y., Dorigny, A., Nicoullaud, B., King, D., Tabbagh, A., 2003. Spatial and temporal monitoring of soil water content with an irrigated corn crop cover using surface electrical resistivity tomography. *Water Resources Res.* 39, 1401-1420.
- McMechan, G.A., Yedlin, M.J., 1981. Analysis of dispersive waves by wave field transformation. *Geophysics* 46, 869-874.
- Miller, R.D., Xia, J., Park, C.B., Ivanov, J.M., 1999. Multichannel analysis of surface waves to map bedrock. *The Leading Edge* 18, 1392-1396.
- Nijland, W., Van der Meije, M., Addink, E.A., De Jong, S.M., 2010. Detection of soil moisture and vegetation water abstraction in a Mediterranean natural area using electrical resistivity tomography. *Catena* 81, 209-216.
- Park, C.B., Miller, R.D., Xia, J., 1999a. Multimodal analysis of high frequency surface waves. In: Proceedings "Application of geophysics to engineering and environmental problems '99", 115-121.
- Park, C.B., Miller, R.D., Xia, J., 1999b. Multichannel analysis of surface waves. *Geophysics* 64, 800-808.
- Park, C.B., Miller, R.D., Xia, J., Ivanov, J., 2000. Multichannel seismic surface-wave methods for geotechnical applications. In: Proceedings of the First Int. Conf. on the App. of Geophys. : Methodologies to Transportation Facilities and Infrastructure, St. Louis, December 11-15.
- Puech, A., Rivoallan, X., Cherel, L., 2004. The use of surface waves in the characterisation of seabed sediments: development of a MASW system for offshore applications. In Proceedings of "Seatech Week, Caractérisation in situ des fonds marins", Octobre 21-24, Brest, France.
- Samyn, K., Cerdan, O., Grandjean, G., Cochery, R., Berndardie, S., Bitri, A., 2011. Assessment of vulnerability to erosion : digital mapping of a loess cover thickness and stiffness using spectral analysis of seismic surface-waves. Manuscript 6540 Geoderma, under review.
- Schenk, H.J., Jackson, R.B., 2002. Rooting depths, lateral root spreads, and belowground/aboveground allometries of plants in water-limited environments. *Journal of Ecology* 90, 480-494.
- Shenk, H.J., 2008. Soil depth, plant rooting strategies and species niches. *New Phytologist* 178, 223-225.
- Soar, C.J., Loveys, B.R., 2007. The effect of changing patterns in soil-moisture availability on grapevine root distribution, and viticultural implications for converting full-cover

irrigation into a point-source irrigation system. Australian J. of Grape and Wine Res. 13, 2-13.

Srayeddin, I., Doussan, C., 2009. Estimation of the spatial variability of root water uptake of maize and sorghum at the field scale by ERT. Plant Soil 319,185-207.

Sturtevant, K. A., Baker, G. S., Snyder, C., Kopczynski, S., 2004. Hydrogeophysical characterization of bedrock fracture orientations using azimuthal seismic refraction tomography. AGU, H23A-1122.

Tarantola, A., 1987. Inverse problem theory. Elsevier Science Publishing Co., Inc., New York.

Tassinari, C., Lagacherie, P., Bouzigues, R., Legros, J.P., 2002. Estimating soil water saturation from morphological soil indicators in a pedologically contrasted Mediterranean region. Geoderma 108, 225-235.

Telford, W.M., Geldart, L.P., Sheriff, R.E., 1990. Applied Geophysics, 2nd ed, Cambridge University Press, Cambridge.

Trambouze, W., Voltz, M., 2001. Measurement and modelling of the transpiration of a Mediterranean vineyard. Agric. and For. Meteorology 107, 153-166.

Xia, J., Miller, R.D., Park, C.B., 1999. Configuration of near surface shear wave velocity by inverting surface wave. In: Proceedings "Application of geophysics to engineering and environmental problems '99", 95-104.

Ziadat, F.M., 2010. prediction of soil depth from Digital terrain data by integrating statistical and visual approaches. Pedosphere 20, 361-367.

Zhou, W., Beck, B.F., Stephenson, J.B., 2000. Reliability of dipole-dipole electrical resistivity tomography for defining depth to bedrock in covered karst terranes. Environmental Geology 39, 760-766.

hal-00657824, version 1 - 9 Jan 2012

1
2
3
4
5
6
7
8
9
10
11
12
13
14
15
16
17
18
19
20
21
22
23
24
25
26
27
28
29
30
31
32
33
34
35
36
37
38
39
40
41
42
43
44
45
46
47
48
49
50
51
52
53
54
55
56
57
58
59
60
61
62
63
64
65

FIGURE CAPTIONS

Figure 1 : Schematic soil toposequence of the study area.

Figure 2 : Experimental design.

Figure 3 : a) Example of a seismic record; b) *c-f* image calculated from the example seismic record, the extracted dispersion curve overlays the image in black dots; c) comparison between observed (black dots) and computed (red solid line) dispersion curves after inversion process. Both dispersion curves are well fitted; d) obtained 1D vertical Vs model after inversion process.

Figure 4 : a) Example of bedrock delimitation from a punctual analysis of a diachronic ERT data; b) Example of bedrock delimitation from a punctual analysis of a seismic data point .

Figure 5 : Representation of the observed bedrock depth and the groundwater level from boreholes and piezometers.

Figure 6 : Resistivity values according to the observed lithologies at the boreholes locations; Black lines represent means and standard deviations, coloured bars represent minimum and maximum resistivity values.

Figure 7: Plot of predicted BD against observed BD at the locations of the boreholes from a) ERT analysis and b) MASW analysis; Triangles represent BD with observed groundwater ; Circles represent BD with no observed groundwater.

Figure 8 : Plot of predicted BD from the combination of ERT and MASW analysis against observed BD.

Figure 9 : BD prediction along the geophysical transects using ERT and MASW combination. Predicted BD is roughly consistent with observed BD on the all transects.

hal-00657824, version 1 - 9 Jan 2012

Figure 1
[Click here to download high resolution image](#)

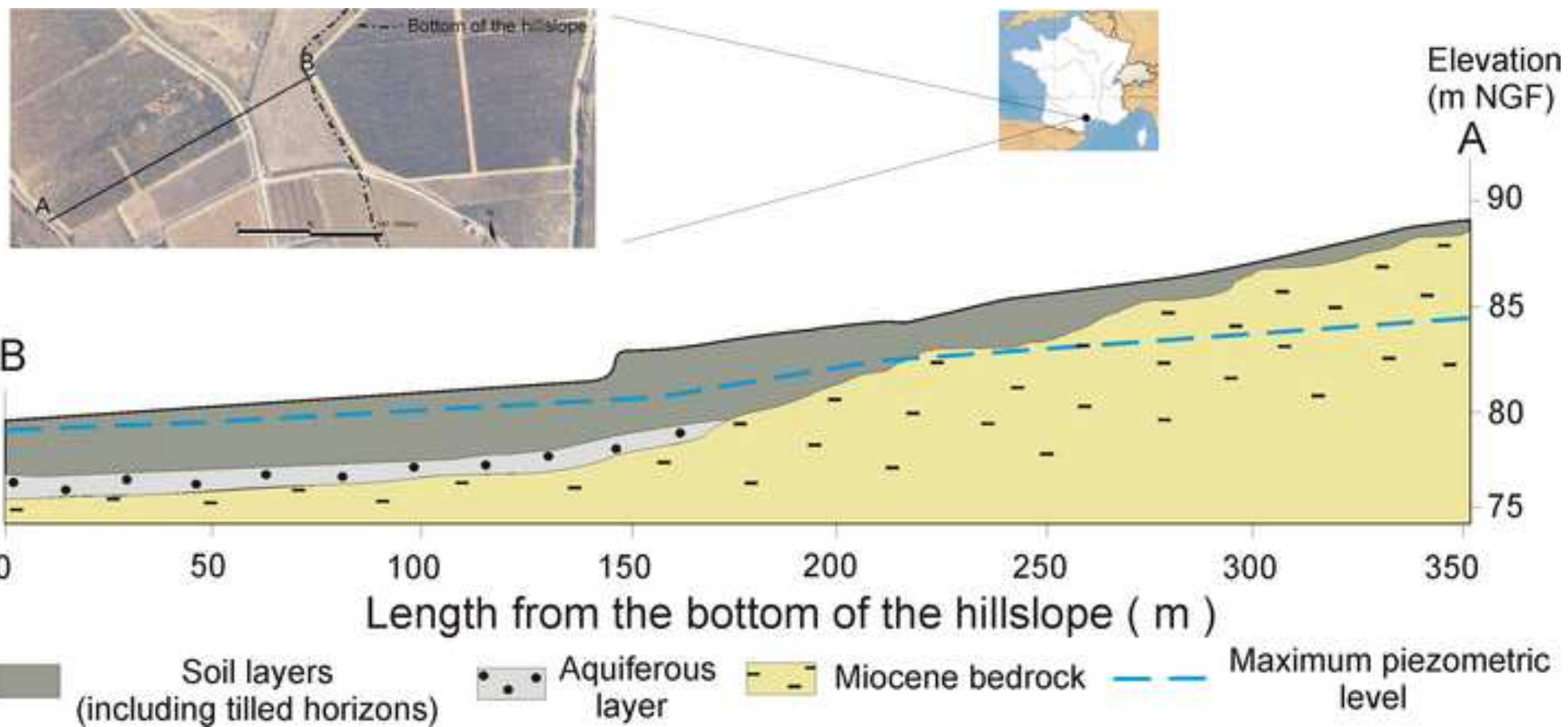


Figure 2
[Click here to download high resolution image](#)

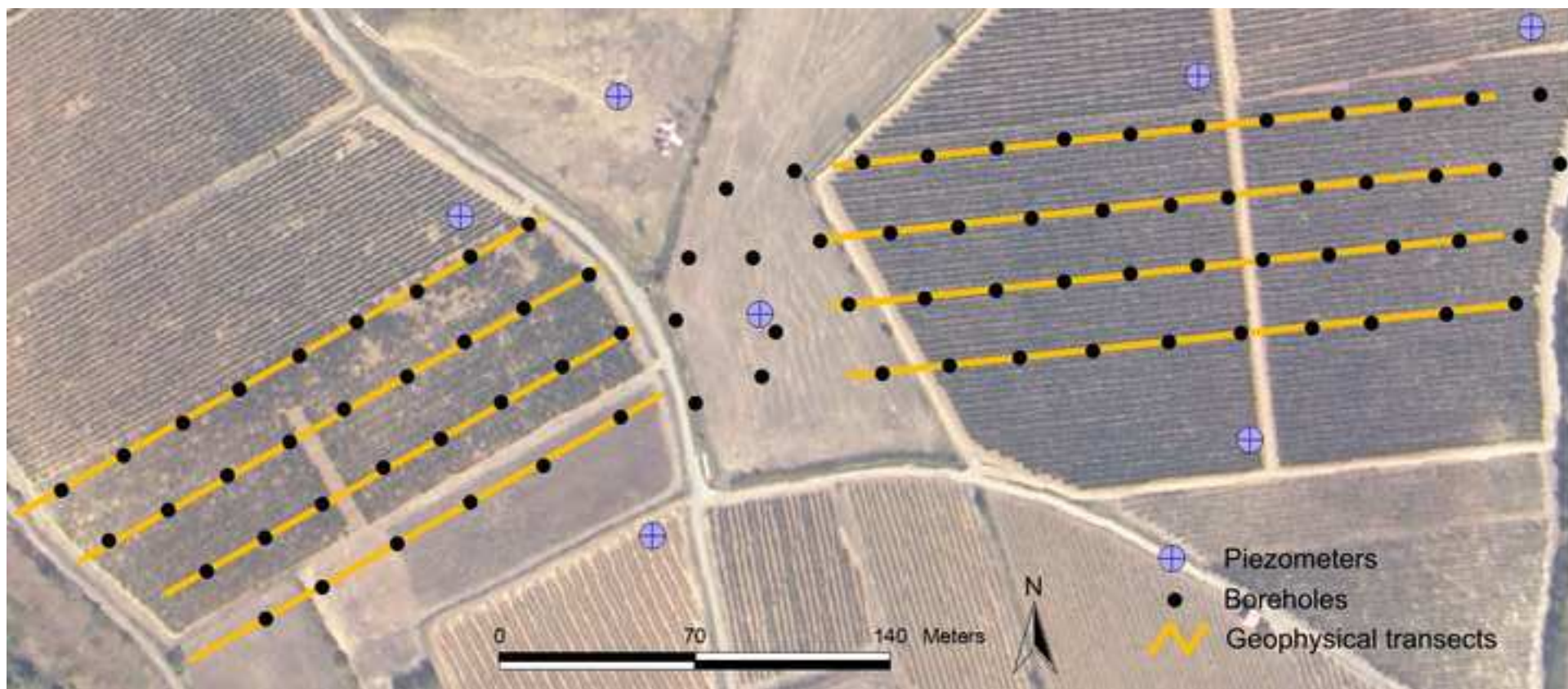


Figure 3
[Click here to download high resolution image](#)

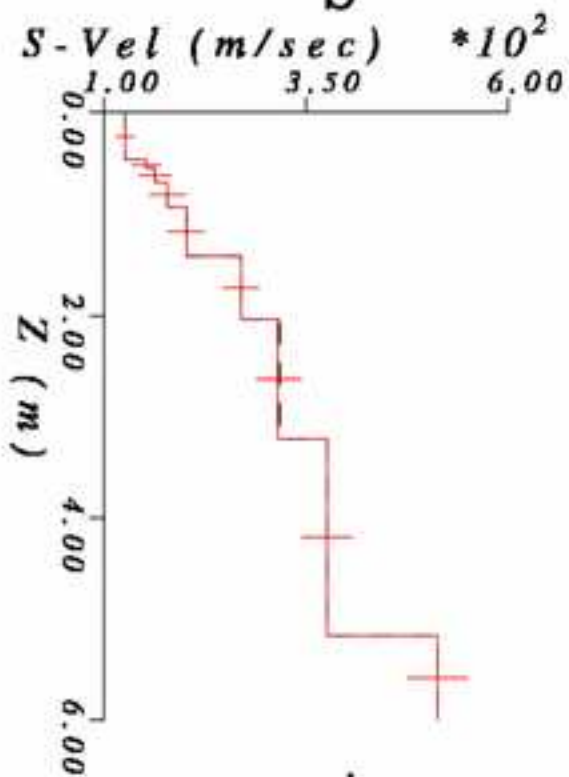
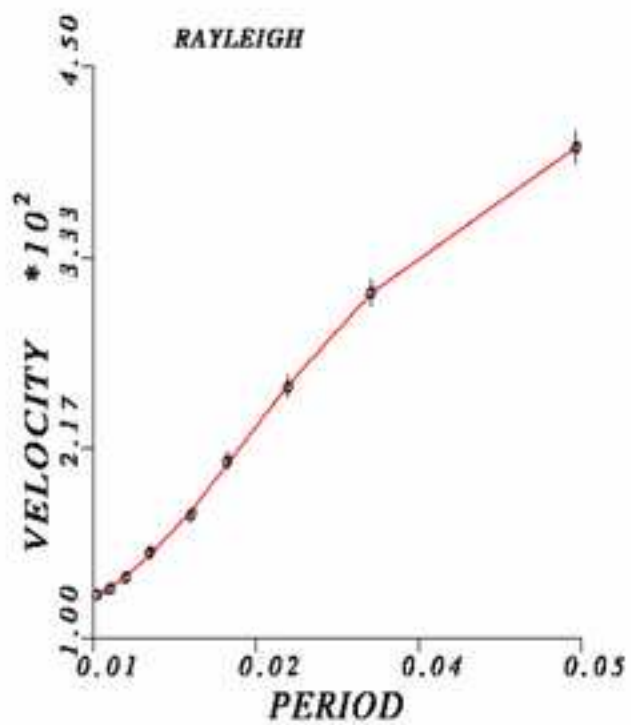
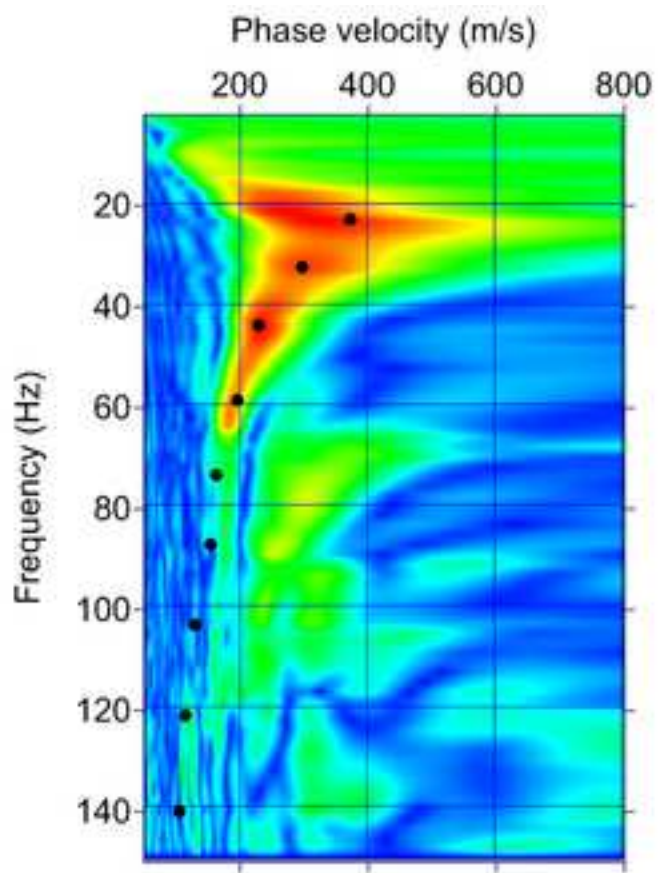
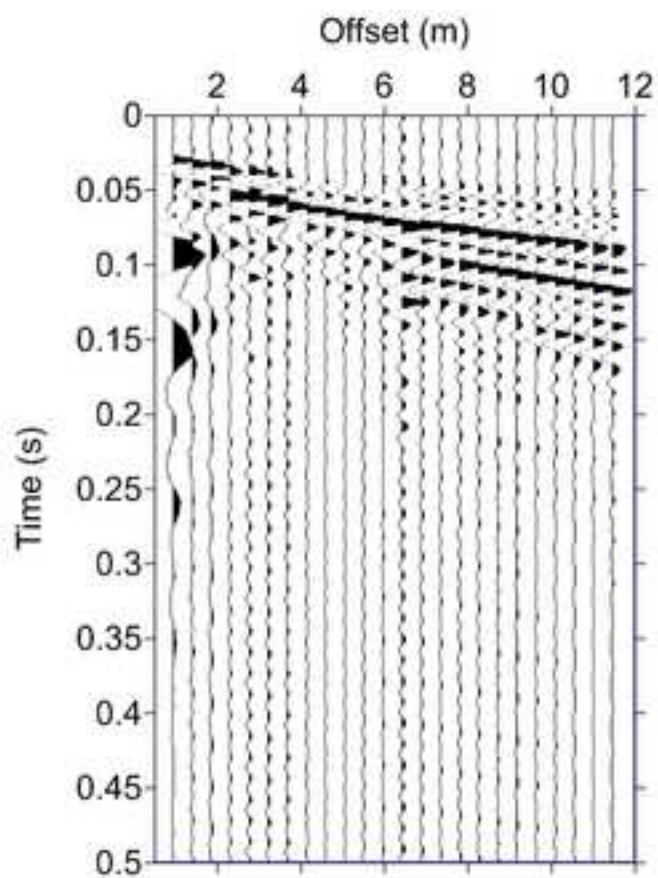


Figure 4
[Click here to download high resolution image](#)

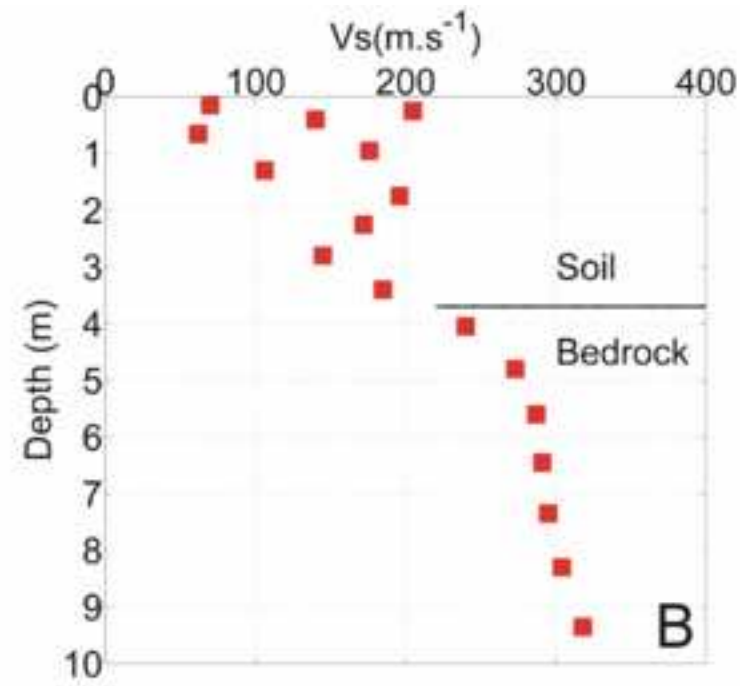
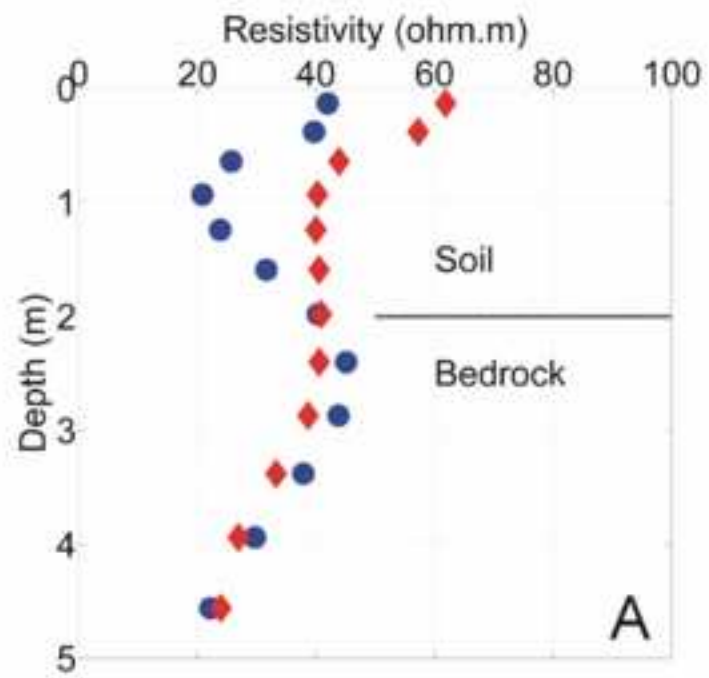


Figure 5
[Click here to download high resolution image](#)

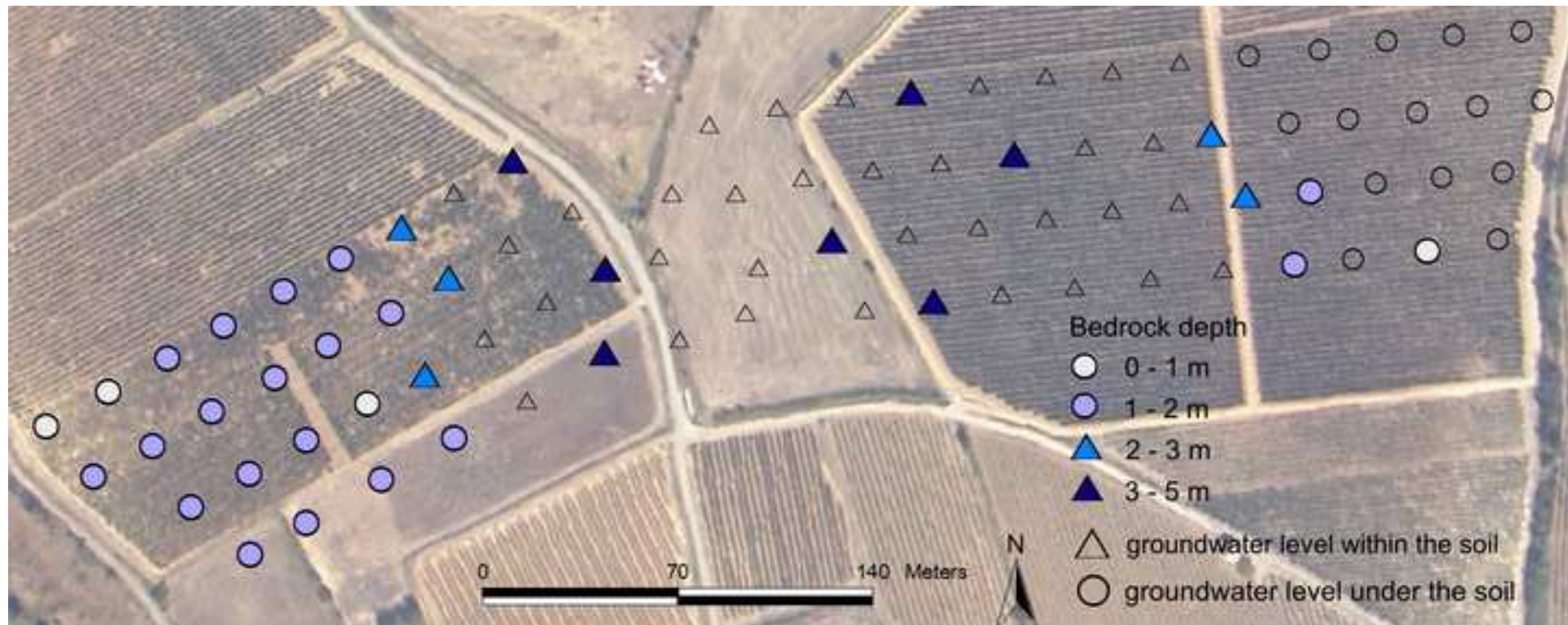


Figure 6

[Click here to download high resolution image](#)

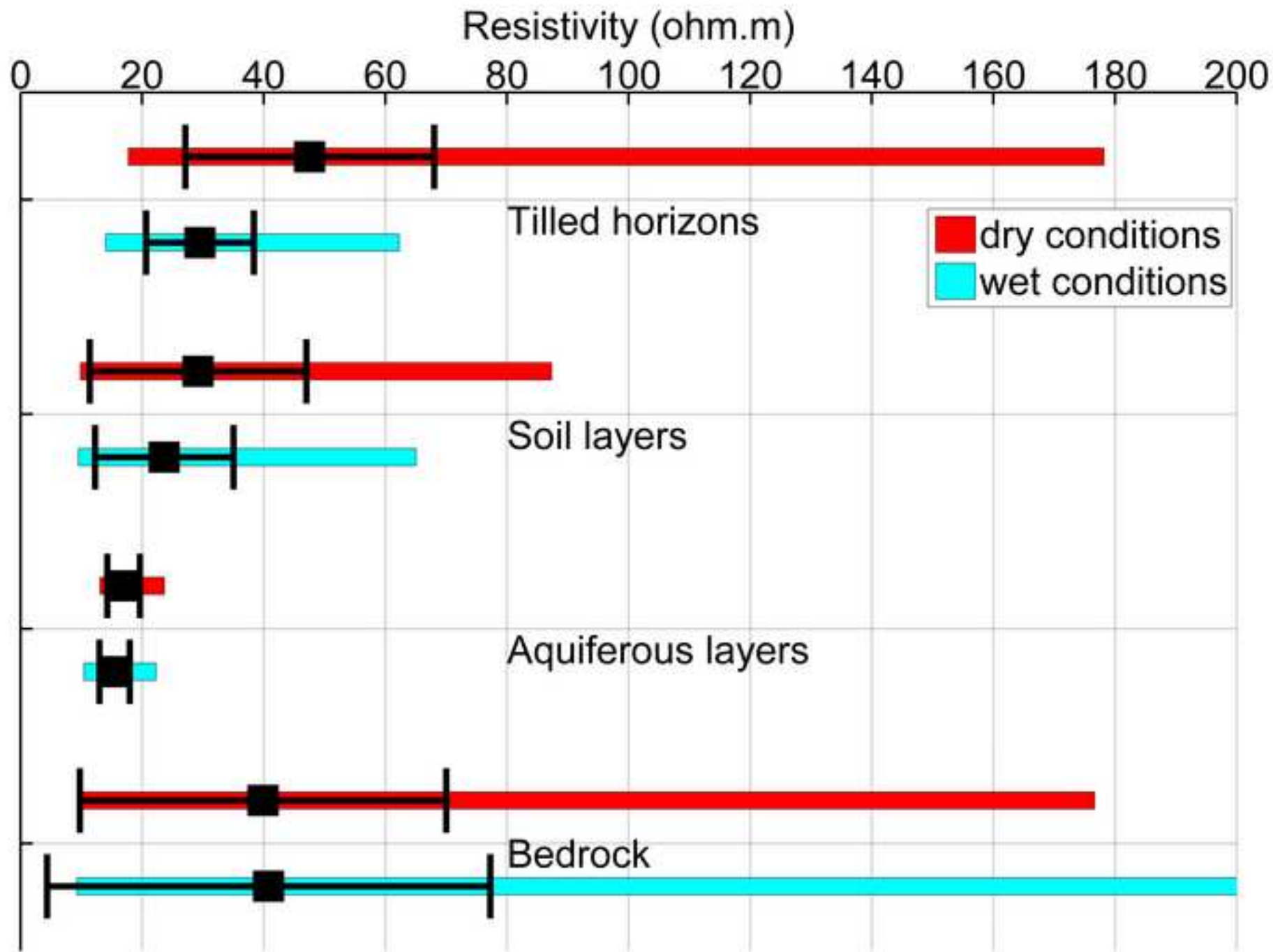


Figure 7
[Click here to download high resolution image](#)

hal-00657824, version 1 - 9 Jan 2012

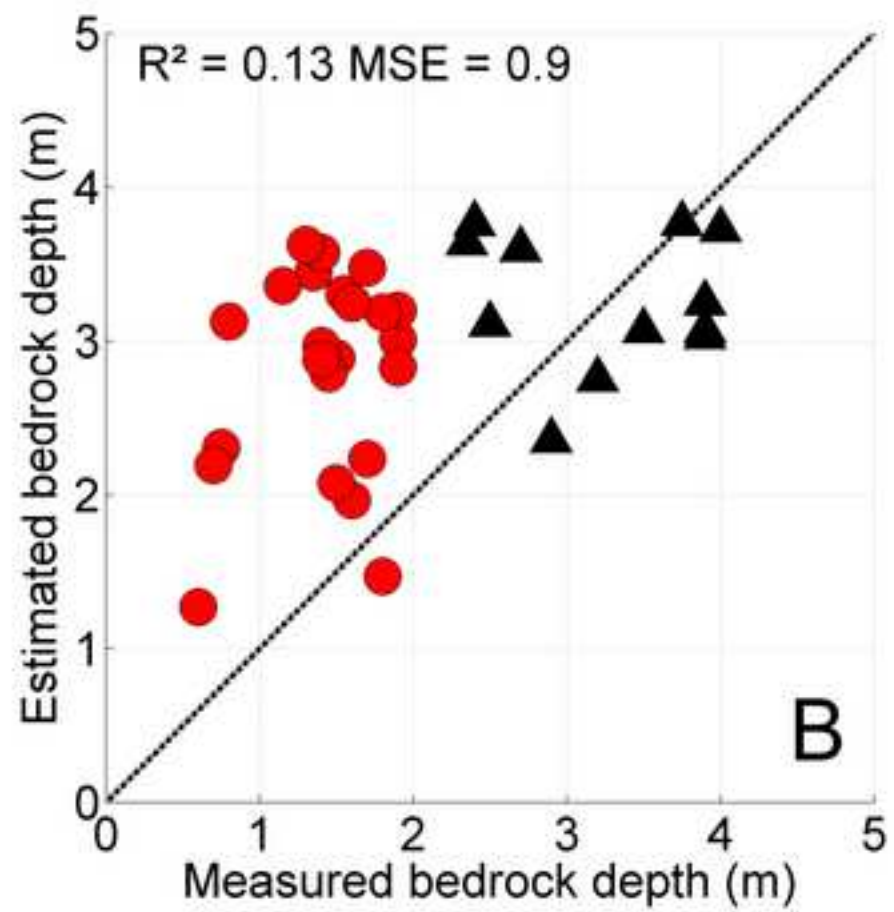
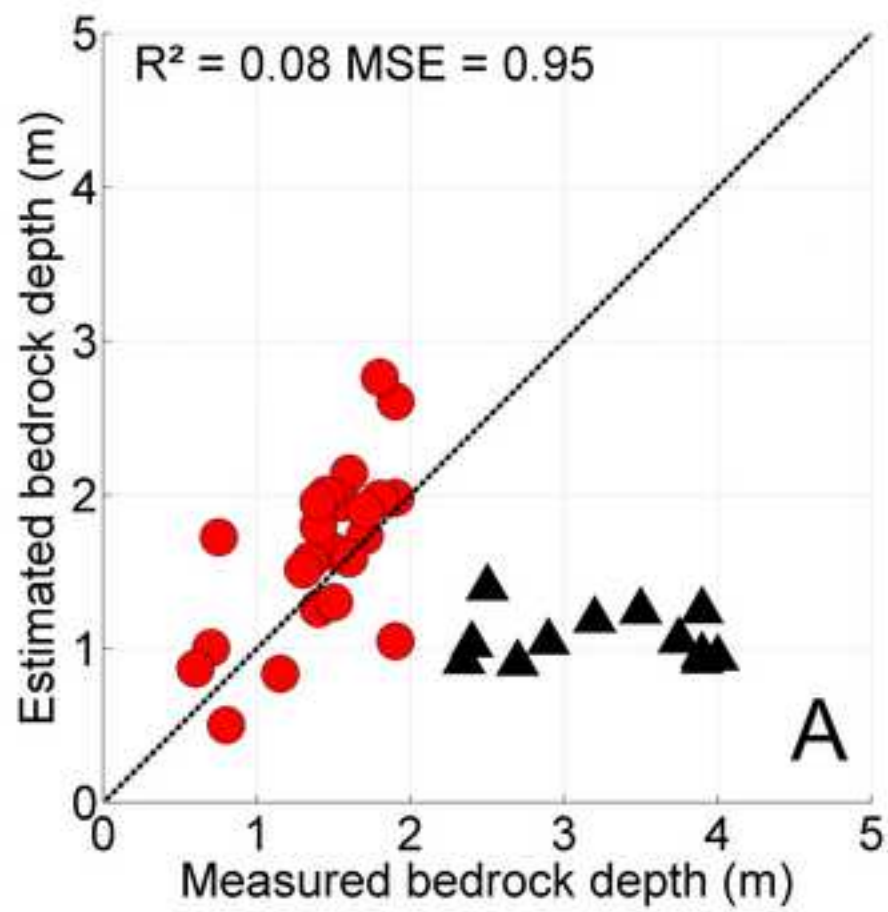


Figure 8
[Click here to download high resolution image](#)

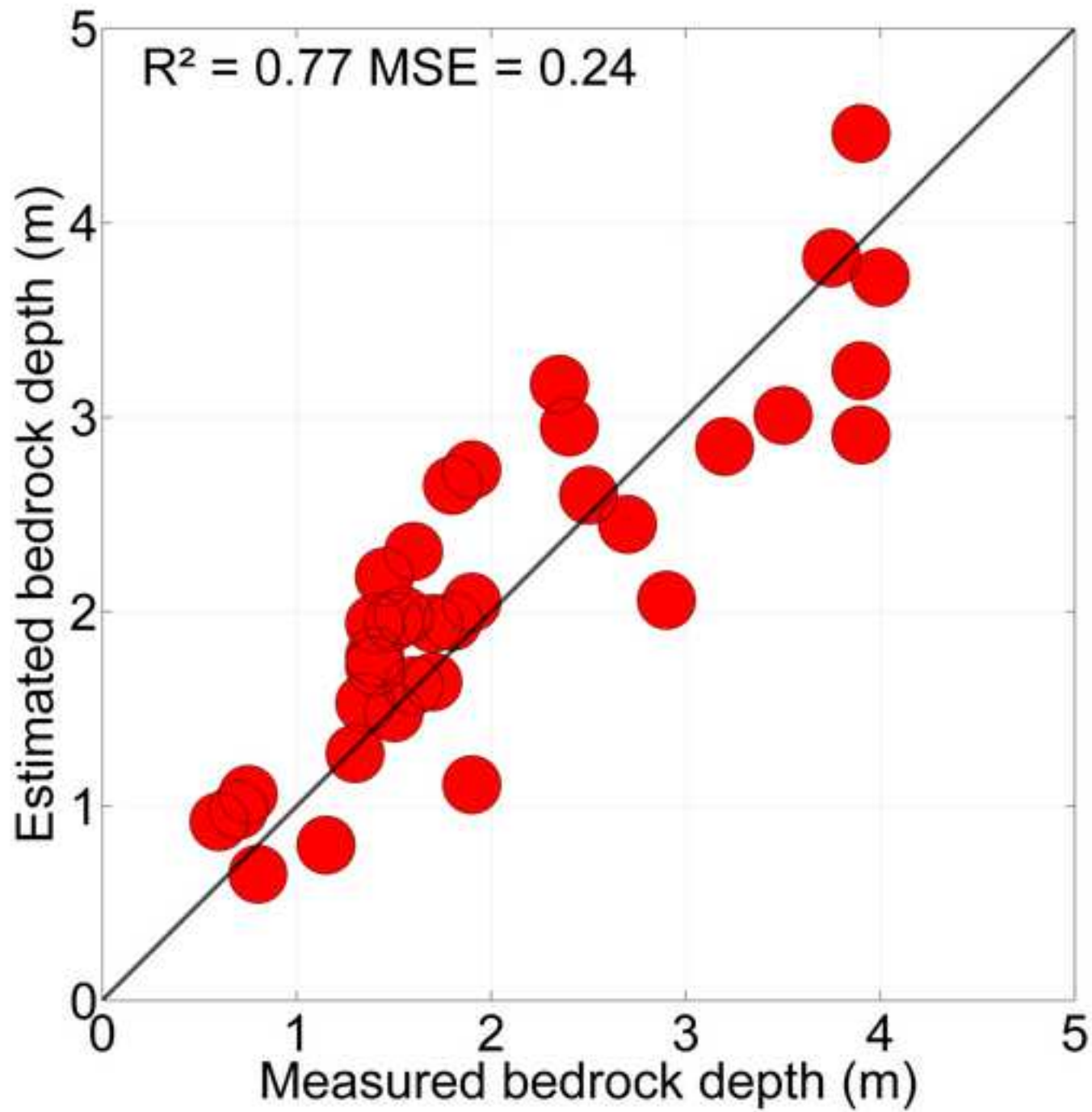
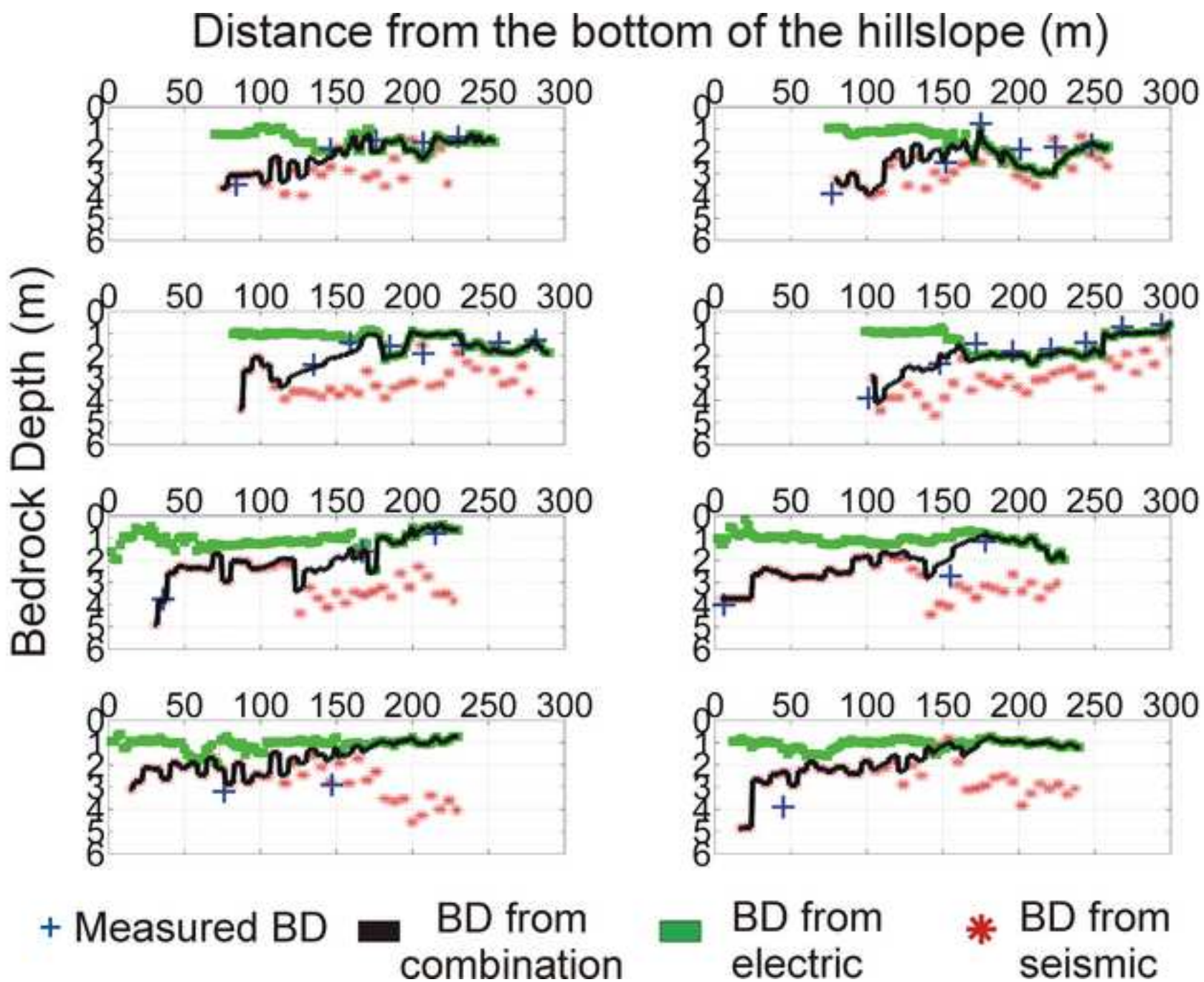


Figure 9
[Click here to download high resolution image](#)



TABLES

Table 1: Chemical and physical analysis of the main soils along the toposequences

*according to Guidelines for soil description, FAO, 2006

** particle size <2 µm for A, 2-50 µm for L and 50-2000 µm for S

Properties	Horizon*	Depth (m)	Colour*	Structure*	Texture**			CaCO3 g/kg
					A	L	S	
Calcisol (in the middle part of the hillslope)	Hp	0 – 0.50	7.5YR44	BS	31	33	36	88
	Bk	0.50 – 1.35	2.5Y64	BS	21	53	26	376
	C	1.35 – 1.60	2.5Y66	BS	16	57	27	411
	Bedrock	>1.60	2.5Y66	Layered	7	21	72	240
Endogleyic	Hp	0 – 0.80	10YR44	BS	19	27	54	119
Calcisol (in the bottom part of the hillslope)	B	0.80 – 1.20	10YR43	BS	26	30	44	7
	Br	1.20 - 1.95	2.5Y53	AB	30	32	38	63
	Bk	1.95 – 2.40	2.5Y53	BS	24	35	41	308
	Bedrock	>2.40	2.5Y63	Layered	18	37	45	281

*according to Guidelines for soil description, FAO, 2006

** particle size <2 µm for A, 2-50 µm for L and 50-2000 µm for S